WETTABILITY CHARACTERIZATION BY NMR T_2 MEASUREMENTS IN EDWARDS LIMESTONE ROCK

E.B. Johannesen[1], H. Riskedal[1], L. Tipura[1], J.J. Howard[2] and A. Graue[1]
[1]University of Bergen, [2]ConocoPhillips

This paper was prepared for presentation at the International Symposium of the Society of Core Analysts held in Calgary, Canada, 10-12 September, 2007

ABSTRACT

Earlier studies on homogenous water-wet chalk core samples showed that Nuclear Magnetic Resonance (NMR) relaxation measurements provide a quantitative and fast technique for determining mixed wettability in laboratory core plugs. This study was extended to include heterogeneous limestone core samples at different oil-wet and water-wet conditions. NMR T_2 relaxation properties for oil- and water-saturated outcrop limestone were measured using the CPMG sequence at various wettabilities and at various fluid saturations during imbibition to find trends for wettability characterization. Several trends were observed. The T_2 relaxation time for the oil phase at irreducible water saturation, S_{wi}, was observed to decrease almost linearly for more oil-wet conditions. For strongly water-wet conditions, T_2 relaxation time for oil as a function of increasing water saturation during spontaneous imbibition was observed to shift to slower relaxation time, and the relative shift decreased for less water-wet conditions. For oil-wet conditions, T_2 relaxation time for oil as a function of increasing oil saturation during spontaneous imbibition was observed to shift to slower relaxation time, and the relative shift increased for more oil-wet conditions.

INTRODUCTION

Wettability

Wettability is defined as "the tendency of one fluid to spread on or adhere to a solid surface in the presence of other immiscible fluids" (Craig, 1971). Salathiel (1973) introduced mixed wettability in which the oil-wet surface form continuous paths for oil through the large pores and smaller pores remain water-wet. Wettability affects capillary pressure, relative permeability and residual oil saturation (Anderson, 1986, 1987a, 1987b, 1987c, 1987d, 1987e). The interaction between rock, brine and crude oil was extensively studied by Buckley et al. (1997, 1998) and the wettability alteration was found to be dependent on aging time, temperature, water saturation, the acid/base number, the compositions of crude oil and water and rock surface, Morrow et al. (1994), Graue et al. (1994), Jadhunandan and Morrow (1995), Zhou et al. (2000).

NMR as a Tool to Measure Wettability

The wettability conditions in a porous media containing two or more immiscible fluid phases determine the microscopic fluid distribution in the pore network. Nuclear Magnetic Resonance measurements are sensitive to wettability because of the strong effect that the solid surface has on promoting magnetic relaxation of the saturating

fluid. The idea of using NMR as a tool to measure wettability was presented by Brown and Fatt (1956). They based their theory on the hypothesis that, at the solid-liquid interface, molecular motion is slower than in the bulk liquid. In this solid-liquid interface the diffusion coefficient is reduced, which in turn is equivalent to a zone of higher viscosity. In the zone of higher viscosity the magnetically aligned protons can more easily transfer their energy to their surroundings. The magnitude of this effect depends upon the wettability characteristics of the solid with respect to the liquid in contact with the surface. Brown and Fatt started their work by measuring proton spin-lattice relaxation time of water in uncoated sand packs as water-wet media, and Dri-film treated sand packs as oil-wet porous media. Their experiments resulted in a linear relation between relaxation rate and fractional oil wetted surface area.

Theory of Relaxation Time Distribution in Porous Media

Microscopically the volume of a single pore in a porous media may be divided into two regions; surface area S and bulk area V (Figure 1). The surface area is a thin layer with thickness δ of a few molecules close to the pore wall surface. The bulk area is the remaining part of the pore volume and usually dominates the overall pore volume. With respect to NMR excitations of nuclear states for hydrogen-containing molecules in these regions, different relaxation times for the induced excited energy states are expected. The relaxation time is significantly faster for a molecule in the surface area, compared to a molecule in the bulk area. This is an effect of paramagnetic centres in the pore wall surface that causes the relaxation time to be faster, as reported by Brown and Fatt (1956).

The inverse of the relaxation time, T_i, is expressed by contributions from the bulk area V, the surface area S and the self diffusion d:

$$\frac{1}{T_i} = \left(1 - \frac{\delta \cdot S}{V}\right)\frac{1}{T_{ib}} + \frac{\delta \cdot S}{V}\frac{1}{T_{is}} + \frac{\left(\gamma G t_E\right)^2 D}{12} \quad i=1,2 \qquad (1)$$

where δ is the thickness of the surface area, S is the surface area, V is the pore volume, T_{ib} is the relaxation time for bulk, T_{is} is the relaxation time for the surface, γ is the gyromagnetic ratio, G is the magnetic field gradient (assumed to be constant), t_E is the time between echoes and D is the self diffusion coefficient of the fluid.

The NMR Signal Intensity in the T_2 distribution plot reflected by the measured amplitude of the NMR signal is proportional to the total amount of hydrogen nuclei, while the relaxation time depends on the interaction between the nuclear spins and the surroundings. In a characteristic pore containing e.g. water, the bulk water exhibits a single exponential decay. The water close to the pore wall surface exhibits faster T_2 relaxation time for this characteristic pore size:

$$\frac{1}{T_i} \approx \rho \frac{S}{V} \qquad (2)$$

where ρ is the surface relaxivity defined as:

$$\rho = \frac{\delta}{T_{iS}} \tag{3}$$

For other pore sizes, the observed T_2 relaxation time will be faster for smaller pores and longer for larger pores. The S/V-ratio can be taken as a measure of pore size.

Due to the pore size variations a non-linear optimization algorithm with multi-exponential terms was used to fit the data, Howard and Spinler (1995). The NMR response is the accumulated response from all individual pore sizes, and the multi-exponential decay may be written as:

$$M(t) = \sum_{i=1}^{n} V_i \exp(-t / T_{2i}) \tag{4}$$

where $M(t)$ is the echo amplitude at time t, T_{2i} is the relaxation time for pores of characteristic size i and V_i is the volume fraction of pores of size i. An advantage of the multi-exponential fitting is that it allows one to predetermine a larger number of T_2 terms that cover the range of interest.

The surface relaxivity, ρ, is influenced by the mineralogic composition of the pore wall surfaces, especially if paramagnetic ions are presented, Dunn et al. (2002). The presence of paramagnetic ions increases the rate of relaxation of the hydrogen atom, Dastidar et al. (2006). From equation (2) both the surface to volume, S/V, and the surface relaxivity, ρ, are unknown parameters. Therefore, T_2 relaxation time is also affected by the pore structure. Apart from mineralogy, there are various other factors that influence the surface relaxivity, ρ, such as experimental procedures and core heterogeneities.

EXPERIMENTAL PROCEDURES

Fluids

Three different crude oils were used as the oil phases during the aging process. Decalin and decane was used after the aging process. Synthetic formation brine was prepared (Table 1).

Core Samples

A total of 14 core samples were cut from the same Edwards Limestone block. The cores had length and diameter of 6 cm and 3.75 cm, respectively.

The core samples were dried in an oven at 90°C for at least 2 days. The dry core samples were vacuum-saturated with brine. Porosity was determined from the change in weight. Absolute brine permeability was measured. Twin core samples with approximately the same porosity and permeability were divided into Group 1-6, to obtain optimum reproducibility (Table 2).

Wettability Alteration

12 core plugs were aged at various length of time at S_{wi} to establish various uniform wettability conditions, Aspenes et al. (2002). Alternate flooding from both ends with crude oil was used at elevated temperature, to obtain chalk core plugs at various mixed wettabilities. The procedure is described by Graue *et al.* (1999, 2002). Only the rock surfaces exposed to crude oil undergo wettability changes during aging. The crude oil used for aging was replaced by decane to establish a stable and reproducible fluid rock system, with a similar mobility ratio at room temperature as experienced in a North Sea reservoir of interest at elevated temperature. The exchange was performed by flushing first five pore volumes of decalin and then five pore volumes of decane through the core plugs. Compared with the work of Graue (1999, 2002) the crude oil has been displaced after five pore volumes. Decalin was used to prevent destabilization of the crude oil.

NMR Measurements

NMR T_2 measurements were obtained at end point water saturation after forced imbibition, S_{orw}, at immobile water saturation, S_{wi}, at different times during oil production by spontaneous oil/water imbibition and at end point oil/water saturation after spontaneous imbibition, S_{wsp}. To initiate the spontaneous oil or water production, the cores were placed in an oil or water bath depending on the process under study. During the spontaneous imbibition, each core plug was taken out of the bath at various selected times and placed in the NMR instrument to measure T_2 relaxation times using the CPMG sequence. Before each NMR measurement the cores were wrapped in a plastic foil to minimize evaporation. Saturations were calculated based on mass balance measurements. The fluid saturations were also found by integrating the NMR response curves for each phase and normalize to the corresponding results at 100% saturations. The saturation results were used to obtain the dynamics for the spontaneous imbibition.

NMR Instrument Parameters Setting

To obtain an optimal T_2 signal from the NMR measurements on limestone, several instrument parameters needed to be investigated. The signal to noise (SN) increased when numbers of scan (NS) increased, and NS was therefore set to 64. Relaxation Delay (RD) was set to 6 s to ensure full polarization between each CPMG sequence. TAU, τ, which is defined as the time between the 90° and the 180° pulse (and 2τ between each 180° pulse) in the CPMG sequence, was investigated for 250 μs and 500 μs to see if diffusion affected the signal. Low τ (250 μs), permits less diffusion than larger τ (500 μs).

Several samples showed dominating diffusion, and τ was therefore preferred to be 250 μs for the experiments. To ensure that all slow components relaxed, the number of echoes (NECH) was set to 4096 for τ = 500 μs and 8100 for τ = 250 μs, so that the total experiment length exceeded the relaxation times for bulk decane and brine.

Rock Description from NMR T_2 Measurements, Mercury Injection and Thin Sections

It has been demonstrated that NMR relaxation rate is proportional to pore size, Brownstein and Tarr (1979). In the fast diffusion regime, the relaxation rate of fluids is directly proportional to the *S/V*-ration of the pores. Two core samples were saturated with 100% brine and 100% decane, respectively, to study the pore-size distribution for the Edwards limestone rock. NMR is not very sensitive to throat size, and mercury injection curves (MICP) were therefore generated between 3.5 kPa and 414 MPa for three samples to study the pore throats. Cylindrical samples were used to decrease intrusion into surface pores at very low pressures, Howard et al. (1993). Thin sections were prepared to study the pore structure and to estimate the quantity of different pore sizes.

EXPERIMENTAL RESULTS AND DISCUSSION

Core Sample Data

All core sample data are presented in Table 2. Variations in porosity, permeability and S_{wi} indicate the degree of heterogeneity in the core plugs. This may have affected the aging.

Rock Description

T_2 distribution plots for the 100% saturated core samples with brine and decane illustrate the pore-size distribution (Figure 2). These are often compared to the independent pore throat-size measurement by MICP (Howard *et al*., 1993). The constant of surface relaxivity ρ from equation (2) was estimated empirically by scaling the longest T_2 value to the largest pore size measured by MICP. The relaxation time distribution plot was scaled to length units with this relaxativity term (Figure 2). The resultant pore-size distribution plots for the decane- and brine-saturated samples show an almost complete overlap that suggests two similar core samples. The plot indicates a majority of pores with a pore diameter at about 150 μm and some pores with pore diameter at about 40 μm. Some micro pores (~1 μm) are also observed.

The MICP measurements for three samples which illustrate the pore throat radius are shown in Figure 3. All three curves show good overlap, indicating fairly similar pore throats for all samples. Throat distribution is relatively broad, but the majority of pore throats are found at about 2 μm.

The thin sections shown in Figure 4 indicate pore-sizes from micro pores to 2 mm, but no vugs are observed. Spherical pores created by dissolution of the bioclasts are observed. Primary porosity is filled with sparry calcite cement, sparry calcite. Secondary porosity is created by the dissolution of the original fossil fragments. Many of these secondary pores are large with very simple geometry (fr. ex. spheres, cylinders) unlike most primary pores that tend to be complex in shape.

Impact of Wettability on T_2 Relaxation Time Measurements

Strongly Water-Wet Conditions (Group 1)

Strongly water-wet conditions were obtained for core samples that were not exposed to crude oil but only saturated with water and then drained to S_{wi} with decane. The peak at 1000 ms on the relaxation time distributions represents the T_2 relaxation time for decane, while the remaining components represent the water-filled pores (Figure 5a). As water saturation increases during spontaneous imbibition, the mobile decane in the largest pores is quickly displaced by water. The slow relaxation component representing the decane-filled pores shifts slightly towards slower times during water imbibition as its intensity decreases. The shift in the slow relaxation time for decane is better illustrated for the two strongly water-wet samples in Figure 6. The relaxation peak that represents water in the larger pores (> 100 ms) shifts towards slower relaxation times and increases in intensity during imbibition. This indicates the partial filling of the larger pores with water. The small portion of water in the microporosity, ~ 20ms, remains unchanged during imbibition.

Moderately Water-Wet Conditions (Group 2)

Moderately water-wet conditions were obtained for core samples drained to S_{wi} by a light crude oil at elevated temperature with no aging. The core plugs exhibited an Amott index of 0.5. Only a small change in saturation was observed during imbibition of water. Due to small variations in saturation during imbibition of water, there was only a minor shift of the decane T_2 peaks towards slower relaxation times (Figure 5b). The T_2 peaks for water shifted towards slower relaxation time during the imbibition, but not as much as for the strongly water-wet samples in Group 1 (Figure 5a).

Weakly Water-Wet Conditions (Group 3)

Weakly water-wet conditions were obtained for core samples drained to S_{wi} by a light crude oil at elevated temperature and then aged for 53 hours. This was reflected by an Amott index of about 0.1. An insignificant change in water saturation (0.30-0.33) was observed during imbibition of water. The saturations were based on T_2 measurements. Because of almost no change in saturation during the imbibition, there was no noticeable shift of T_2 peaks for decane (Figure 5c). Even with the small saturation change in these samples the T_2 peaks for water moved towards slower relaxation time.

Weakly Oil-Wet Conditions (Group 4)

Weakly oil-wet conditions were generated for core samples drained to S_{wi} by crude oil at elevated temperature and then aged for 192 hours. This was reflected by an Amott index of about -0.1. The saturations were based on T_2 measurements. Most apparent in the T_2 distributions is the shift in the slow decane component from a bulk value of ~ 1000 ms to 700 ms in these samples (Figure 5d). For a weakly oil-wet sample some parts of the pore wall surface may be in direct contact with decane, resulting in decreased T_2 relaxation time. This peak shifted towards slower times during spontaneous imbibition of decane (Figure 5d). The water relaxation component at ~100 ms did not change much in position nor in intensity during decane imbibition.

Weakly to Moderately Oil-Wet Conditions (Group 5)

Weakly to moderately oil-wet conditions were obtained for core samples drained to S_{wi} by oxidized crude oil at elevated temperature and then aged by the oxidized crude oil for 192 hours. The measured Amott index was -0.3. As decane imbibed into the oil-wet pore network the oil film that covered some parts of the pore walls thickened and the S/V-ratio decreased. This resulted in slower T_2 relaxation time for the decane phase from 403 ms to 427 ms. (Figure 5e). T_2 shift for decane was more significant for this weakly to moderately oil-wet sample compared to the weakly oil-wet sample (Figure 5d). The initial water saturation during aging was approximately the same for both the weakly and the weakly to moderately oil-wet samples, and pore wall surfaces exposed to crude oil was the same. The only difference was the crude oil and the aging process.

Moderately Oil-Wet Conditions (Group 6)

Moderately Oil-wet conditions were obtained for core samples drained to S_{wi} with heavy crude oil at elevated temperature and then aged by heavy crude oil for 192 hours. The measured Amott index was -0.5. The water production started immediately after exposing the core samples to decane, which indicated moderately oil-wet conditions. The decane T_2 peaks shifted towards slower times as a function of increasing oil saturation during spontaneous imbibition of decane (Figure 5f). As expected, T_2 relaxation time for the decane component increased more rapidly with increased oil saturation for moderately oil-wet conditions, as an effect of more dominating decane bulk contribution (equation 2). The shifts for the two moderately oil-wet samples are illustrated in Figure 6.

Approximate Wettability Determination on Edwards Limestone Using NMR T_2 Measurements

By comparing all T_2 peaks for decane at S_{wi} with expected/obtained wettability, a trend indicated that NMR T_2 measurements can be used for wettability determination on Edwards Limestone (Figure 7). The T_2 values were normalized to values between 0 and 1, where 1 was the slowest measured T_2 value (Figure 7). A similar result was reported on homogeneous chalk by Johannesen et al. (2006). For strongly water-wet conditions at S_{wi}, a solid water film covered the pore wall surface, and surface relaxation for decane was therefore not dominating. For weakly water-wet conditions, some decane was in direct contact with the pore surface and induced faster surface relaxation for the decane phase. When the limestone was aged to oil-wet conditions, the large pores exposed to the crude oil during aging were oil-wet and the surface relaxation for decane was therefore faster in these pores.

The two oil-wet samples from Group 6 were located over the trend line in Figure 7. The signal intensity for decane at S_{wi} for both samples in Group 6 was noticeably lower than the other signals showed in Figure 7, and it could be due to increased temperature during the measurements. The cores in Group 6 had considerably lower permeability than the cores in Group 5 (which had approximately the same wettability), but the porosity was nearly the same for the two Groups. The low permeability could indicate that more small pores remained strongly water-wet after the aging and gave less

contribution to the surface relaxation. This could result in slower T_2. For smaller pores exposed to crude oil and altered to oil-wet conditions, the S/V-ratio for the decane filled pores was less compared to larger pores, and from equation (2) T_2 for decane would increase. Core plug HR9 from Group 6, marked as "X" in Figure 7, was aged at S_{wi} = 0.35, while the other core plugs were aged at considerable lower water saturation. The high S_{wi} may explain why this core appears as an outlier from the trend curve. Only the larger pores were oil-wet and resulted in increased S/V-ratio for the decane filled pores and increased the T_2 relaxation time for oil. The observed pore geometry from both petrophysical evaluation and geological rock description may therefore explain why the measured T_2 decane values for core samples at the same wettability conditions show some fluctuation.

CONCLUSIONS

- The Edward limestone samples used in this study have a highly heterogeneous pore geometry that affects the aging process and the NMR relaxation measurements. The pore diameters for Edwards limestone samples varied from 1 μm to 2 mm, with a majority of the pores at about 150 μm. The average pore throat radius was about 2 μm.
- NMR T_2 relaxation time of the decane component in the rock at S_{wi} was used for wettability estimate that compared favourably with Amott indices.
- Under strongly water-wet conditions, the T_2 relaxation time of the decane component shifted towards slower relaxation times as a function of increasing water saturation during spontaneous imbibition. The relative shift decreased for less water-wet conditions.
- For oil-wet conditions, T_2 relaxation time for decane was faster than that observed under water-wet conditions. This relaxation peak also shifted towards slower relaxation times as a function of increasing oil saturation during spontaneous imbibition. The relative shift increased for more oil-wet conditions.

ACKNOWLEDGMENTS

One of the authors is indebted for financial support to the Norwegian Research Council.

NOMENCLATURE

D = self diffusion coefficient of fluid, cm^2/s
G = magnetic field gradient, gauss/cm
I_w = Amott Index (wettability index)
S_w = water saturation
S_{or} = residual oil saturation
S_{wi} = non- reducible water saturation
S_{wsp} = end point water saturation after spontaneous imbibition
S_{orw} = end point water saturation after forced imbibition
S = pore surface area, m^2
S/V = pore surface area to volume ratio, m^{-1}
T_1 = spin-lattice relaxation time, s
T_2 = spin-spin relaxation time, s
T_{ib} = relaxation time for pore bulk, ms
T_{is} = relaxation time for pore surface, ms
t_E = time between echoes, ms
V = pore volume, m^3
δ = thickness of pore surface area
γ = gyromagnetic ratio, Mhz/T

REFERENCES

Anderson, W.G.: "Wettability Literature Survey – Part 1: Rock/Oil/Brine Interactions and the Effects of Core Handling on Wettability", JPT (Oct. 1986) 1125-1149.

Anderson, W.G.: "Wettability Literature Survey – Part 2: Wettability Measurement", JPT (Nov. 1986) 1146-1262.

Anderson, W.G.: "Wettability Literature Survey – Part 3: The Effects of Wettability on the Electrical Properties of Porous Media", JPT (Oct. 1987) 1283-1300.

Anderson, W.G.: "Wettability Literature Survey – Part 4: Effects of Wettability on Capillary Pressure", JPT (Oct. 1987) 1453-1468.

Anderson, W.G.: "Wettability Literature Survey – Part 5: Effects of Wettability on Relative Permeability", JPT (Nov. 1987) 1605-1622.

Anderson, W.G.: "Wettability Literature Survey – Part 6: Effects of Wettability on Waterflooding", JPT (Des. 1987) 1605-1622.

Aspenes, E., Graue, A. and Ramsdal, J., "In situ wettability distribution and wetting stability in outcrop chalk aged in crude oil", (2002) *J. Petr. Sci.& Eng.*, **39**, 337-350.

Brown, R.J.S., Fatt, I., "Measurements of Fractional Wettability of Oilfield Rocks by the Nuclear Magnetic Relaxation Method", (1956) *Trans. AIME*, **207**, 262-264.

Brownstein, K.R., Tarr, C.E., "Importance of Classical Diffusion in NMR Studies of Water in Biological Cells", (1979) *Physics Review A,* **19**, 2446-2453.

Buckley, J.S., Liu, Y., Xie, X., Morrow, N., "Asphaltenes and Crude Oil Wetting – The Effect of Oil Composition", (1997) *SPEJ*, SPE35366, 107-119.

Buckley, J.S., Liu, Y., "Some mechanisms of Crude Oil/Brine/Solid Interactions", *Jour. Pet. Sci. & Eng.,* (1998) **20**, 155-160.

Craig, F.F., "The Reservoir Charateristics of Waterflood", (1971) Monograph Series, SPE, Vol.

Dastidar, R., Sondergeld, C.H., Rai, C.S., "NMR Desaturation and Surface Relaxivity Measurements on Clastic Rocks" (2006) SPE 99629.

Dunn, K.J., Bergman, D.J, LaTorraca, G.A., *Nuclear Magnetic Resonance Petrophysical and Logging Applications,* Pergamon, (2002), 312.

Graue, A., Aspenes, E., Bognø, T., Moe, R.W., Ramsdal, J., "Alteration of Wettability and Wettability Heterogeneity", (2002) *J. Petr. Sci.& Eng.*, **33**, 3-17.

Graue, A., Bognø, T., Moe, R.W., Baldwin, B.A., Spinler, E.A., Maloney, D., Tobola, D.P., "Impacts of Wettability on Capillary Pressure and Relative Permeability", (1999) SCA9907.

Graue, A., Tonheim, E. and Baldwin, B., "Control and Alteration of Wettability in Low-Permeability Chalk", (1994) Rev.Proc.: 3rd International Symposium on Evaluation of Reservoir Wettability and its Effect on Oil Recovery, Laramie, Wyoming.

Howard, J.J., Kenyon, W.E., Straley, C., "Proton-magnetic resonance and Pore-size Variations in Reservoir Sandstones", (1993) *SPE Formation Evaluating*, **8**, 3, 194-200.

Howard, J.J., Spinler, E. A., "Nuclear Magnetic Resonance Measurements of Wettability and Fluid Saturations in Chalk", (1995) SPE 26471, Houston.

Howard, J.J., "Quantitative Estimates of Porous Media Wettability from Proton NMR Measurements", (1998) *Magnetic Resonance Imaging*, **16**, 5-6, 529-533.

Jadhunandan, P., Morrow, N.R., "Effect of Wettability on Waterflood Recovery for Crude Oil/Brine/Rock Systems", (1995) *SPERE 10*, **1**, 40-46.

Johannesen, E.B., Steinsbø, M., Howard, J.J. and Graue, A., "Wettability Charaterization by MNR T_2 Measurements in Chalk", (2006) SCA0639.

Morrow, N.R., "Wettability and its Effect on oil Recovery", (1990) *JPT* , 1476-1484.

Morrow, N.R., Ma, S., Zhou, X., Zhang, X., "Characterization of Wettability from Spontaneous Imbibition Measurement", (1994) paper CIM 94-47, Proc.: 1994 Petr. Soc. of CIM Ann. Tech. Meeting and AOSTRA 1994 Ann. Tech. Conf., Calgary June 12-15.

Salathiel, R.A., 1973. "Oil recovery by surface film drainage in mixed-wettability rocks", (1973) *Journal of Petroleum Technology*, 1216-1224.

Zhou, X., Morrow, N.R., Ma, S., "Interrelationship of Wettability, Initial Water Saturation, Aging Time and Oil recovery by Spontaneous Imbibition and Waterflooding", (2000), *SPE Journal,* **5**, 2, 199-207.

Table 1. Fluid data.

Fluid	Type/Content	Viscosity at 20°C,[cP]	Density at 20°C,[g/cm^3]
Brine	Distillate water 5 wt. % NaCl 5 wt. % $CaCl_2$ 0.01 wt. %NaN_3	1.057	1.09
Crude Oil B	0.90 wt. % asphaltenes 53 wt. % saturated hydrocarbons 35 wt. % aromatics 12 wt. % NSO containing components Acid number: 0.09 Base number: 1.179	0.85	14.3
Crude Oil D	0.008 wt. % asphaltenes 82.6 wt. % saturated hydrocarbons 14.80 wt. % aromatics 2.54 wt. % NSO containing components Acid number: 0.00 Base number: 0.11	2.06	0.79
Heavy Crude Oil	No chemical analysis		
n-Decane ($C_{10}H_{22}$)	Mineral oil	0.73	0.92
Decahydronaphtalene (Decalin, $C_{10}H_{18}$)	Mineral oil	0.90	0.85

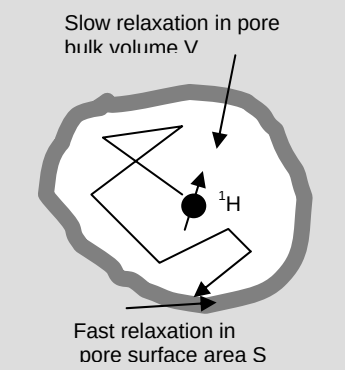

Figure 1. Nuclear spin relaxation properties in a pore divided into bulk volume *V* and pore surface *S*.

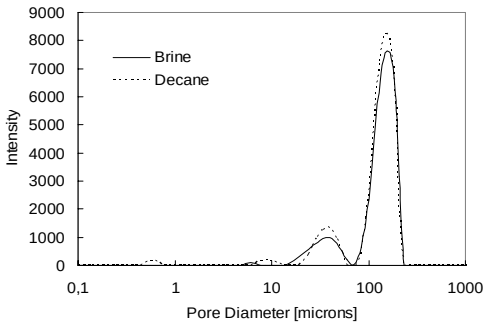

Figure 2. Pore size distribution from NMR T_2 measurements; one core sample 100% brine saturated and one core 100% decane saturated.

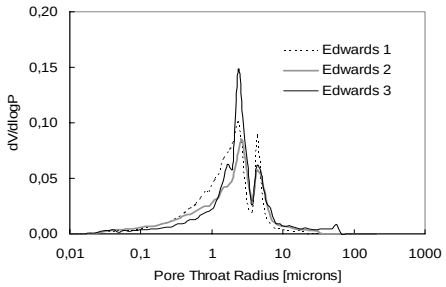

Figure 3. Pore throat radius of three samples measured by MICP that shows a broad distribution of throats.

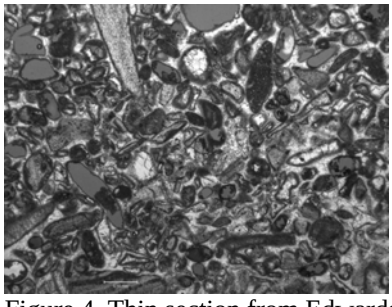

Figure 4. Thin section from Edwards limestone that illustrates large variability in pore sizes and shapes (black) and grains (shades of grey).

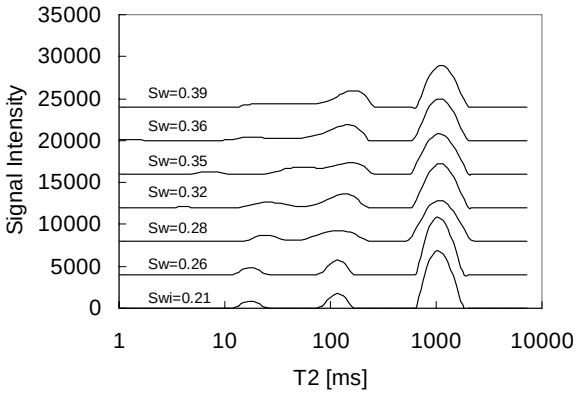

a. Strongly water-wet (LT2)

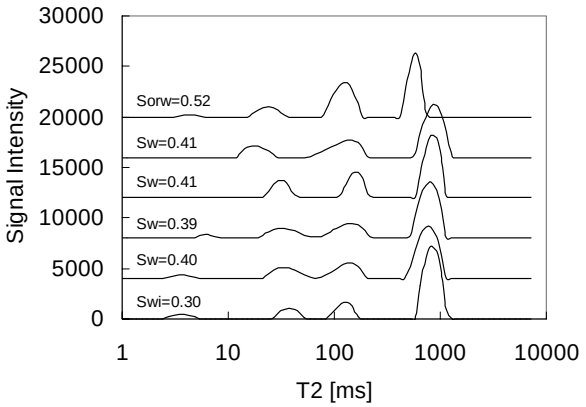

b. Moderately water-wet (HR12)

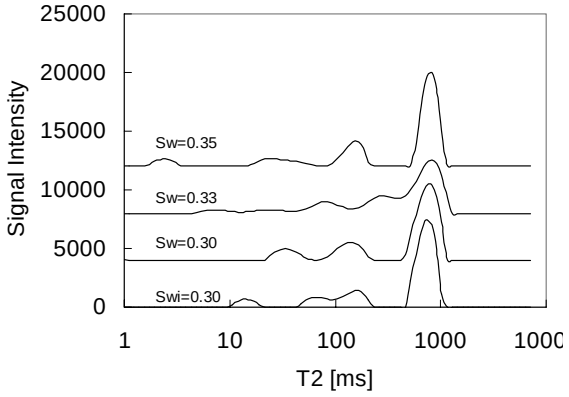

c. Weakly water-wet (HR13)

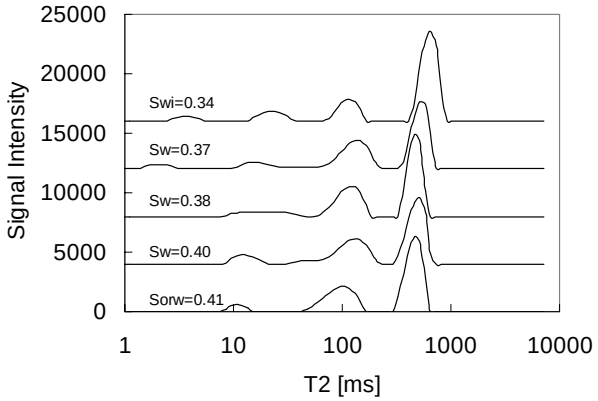

d.Weakly oil-wet (LT1)

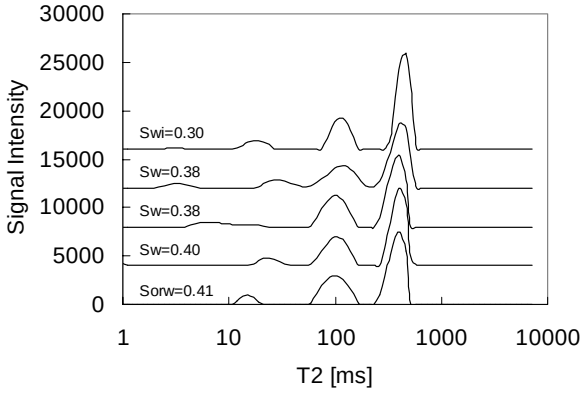

e. Moderately oil-wet (LT5)

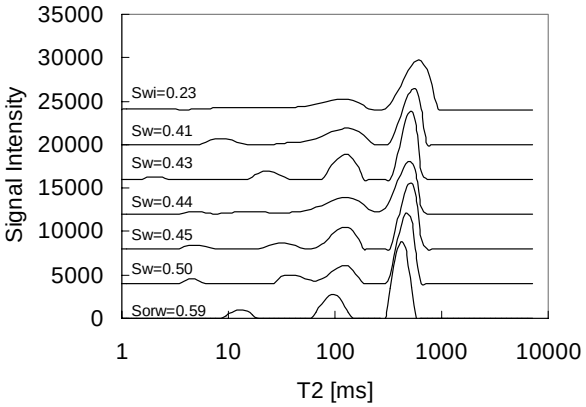

f. Oil-wet (HR11)

Figure 5. T_2 distribution for six core plugs at different wettability conditions at different saturations during spontaneous imbibition of brine and oil.

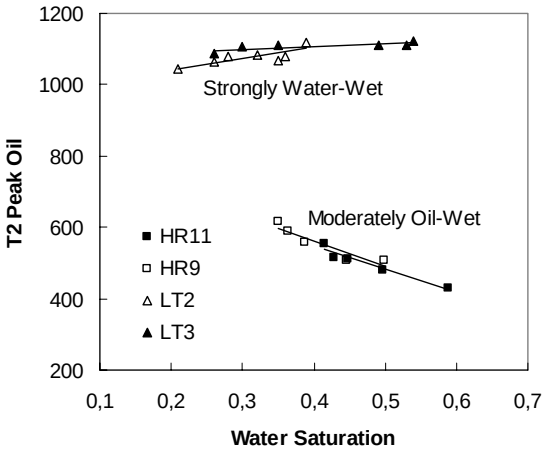

Figure 6. Shift in T_2 peaks for the oil phase as a function of water saturation during spontaneous imbibition of oil for the two moderately oil-wet samples (HR11 and HR9) and spontaneous imbibition of water for the two strongly water-wet samples (LT2 and LT3).

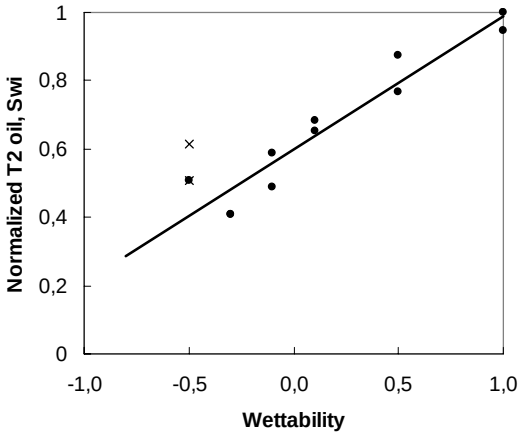

Figure 7. Normalized T_2 peaks for the oil phase at S_{wi} versus expected/obtained wettability for all core samples. The cross represents core plug HR9.

Table 2. Core plugs data.

Core Plug	Group	Porosity	Abs. Perm. [mD]	Crude Oil	Aging Time [h]	Swi (before aging)	Amott Index
LT2	1	0,22	10,9		0	0,21	1
LT3	1	0,22	2,6		0	0,26	1
HR12	2	0,18	7,6	D (light oil)	0	0,29	0,5
HR7	2	0,19	6,5	D (light oil)	0	0,24	0,5
HR13	3	0,23	13,4	D (light oil)	53	0,25	0,1 *
HR14	3	0,23	12,5	D (light oil)	53	0,23	0,1 *
LT1	4	0,20	6,3	oil B	192	0,25	-0,1 *
LT6	4	0,19	7,1	oil B	192	0,21	-0,1 *
LT4	5	0,24	21,4	oxidized oil B	192	0,22	-0,3
LT5	5	0,23	18,7	oxidized oil B	192	0,24	-0,3
HR11	6	0,21	9,0	20 % heavy oil, 80 % oil B	180	0,21	-0,5
HR9	6	0,23	8,9	20 % heavy oil, 80 % oil B	180	0,35	-0,5

* The Amott test is not completed yet, but assumption of wettability conditions is based on previous experiments with the same oil/brine/rock system.